Angular Correlation Studies of Electric Field Gradients in Dilute Silver Alloys*

GEORGE W. HINMAN,† GILBERT R. HOY,‡ JOSEPH K. LEES,§ AND JOHN C. SERIO
Carnegie Institute of Technology, Pittsburgh, Pennsylvania
(Received 29 October 1963)

Measurements of the angular correlation of cascade gamma rays have been used to investigate electric field gradients at lattice sites in dilute silver alloys. The field gradients arise from the redistribution of conduction electrons around solute atoms (valence effect) and from the distortion of the host lattice by these atoms (size effect). The results indicate that the valence effect is predominant but that the size effect can be comparable in magnitude in some cases.

I. INTRODUCTION

UNTIL recently the Thomas-Fermi model[1] was used to describe the electron screening around solute atoms in a metal. However, experiments done in the past several years have shown that the Thomas-Fermi model is inadequate to explain certain observed long-range effects.[2–5] A number of calculations[5–7] have been made that predict such effects and these results have been used to explain the experiments. A characteristic feature of both experiment and calculation is that the electric field gradient in the vicinity of a solute atom is closely related to the valence difference between host and solute.

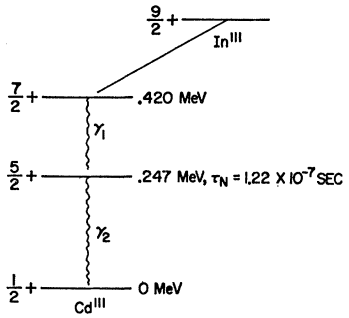

FIG. 1. Simplified decay scheme of In^{111}.

It has always been recognized that there may also be a contribution to the electric field gradient resulting from distortion of the host lattice by the solute atoms, but direct correlation of experimental data with the change in lattice parameter caused by solute addition has been very poor. Sagalyn, Paskin, and Harrison[8] have nevertheless recently considered the size effect in analyzing Rowland's[2] data. Their results indicate that lattice distortions in dilute copper alloys may make a significant contribution to the total electric field gradient.

In the present paper a series of measurements made on dilute silver alloys is described and an investigation is carried out of the relative importance of size and valence contributions to the field gradient.

II. DESCRIPTION OF EXPERIMENTS

In the present experiments, the effects of electric field gradients near solute sites in the lattice are measured by introducing nuclear "probes" into dilute alloys of silver. The probes are radioactive In^{111} nuclei produced in the lattice by α-particle bombardment of the alloys, the reaction being $Ag^{109}+\alpha \rightarrow In^{111}+2n$. The experimental method consists in measuring the angular correlation of the two cascade gamma rays from the decay of the probe nuclei. The decay scheme of In^{111} is shown in Fig. 1. In the absence of any perturbation, the relative probability that the emission direction of the second gamma ray in the cascade makes the angle ϑ with that of the first is

$$W(\vartheta)=\sum_{\text{even } k} A_k P_k(\cos\vartheta)\,, \qquad (1)$$

with the conventional normalization of W taken as $A_0=1$. For the gamma cascade in this experiment, Steffen[9] has measured the values $A_2=-(0.180\pm0.002)$ and $A_4=0.002\pm0.003$. In the following, A_4 is taken to be zero, so that $W(\vartheta)=1+A_2P_2(\cos\vartheta)$. This is consistent with Steffen's result. When the intermediate state is perturbed, the expression for $W(\vartheta)$ is modified.[10] Under certain very general conditions, the presence of a perturbation introduces into each term of Eq.

* This work was supported by the National Science Foundation.
† Present address: General Atomic Division, General Dynamics Corporation, San Diego, California.
‡ Portions of this paper are taken from a thesis submitted by this author to Carnegie Institute of Technology in partial fulfillment of the requirements for the degree of Doctor of Philosophy.
§ National Science Foundation predoctoral fellow.
[1] N. F. Mott, Proc. Cambridge Phil. Soc. **32**, 281 (1936).
[2] N. F. Bloembergen and T. J. Rowland, Acta Met. **1**, 731 (1953); T. J. Rowland, Phys. Rev. **119**, 900 (1960); **125**, 459 (1962).
[3] C. A. Giffels, G. W. Hinman, and S. H. Vosko, Phys. Rev. **121**, 1063 (1961); G. W. Hinman, G. R. Hoy, and J. K. Lees, J. Phys. Soc. Japan Suppl. II **18**, 54 (1963).
[4] Alfred G. Redfield, Phys. Rev. **130**, 589 (1963).
[5] A. Blandin and J. L. DePlante, J. Phys. Radium **23**, 609 (1962).
[6] J. Friedel, Phil. Mag. **43**, 153 (1952); *Advances in Physics*, edited by N. F. Mott (Taylor and Francis, Ltd., London, 1954), Vol. 3, p. 446; Nuovo Cimento Suppl. **2**, 287 (1958); A. Blandin, E. Daniel, and J. Friedel, Phil. Mag. **4**, 180 (1959); A. Blandin and E. Daniel, Phys. Chem. Solids **10**, 126 (1959); A. Blandin and J. Friedel, J. Phys. Radium **21**, 689 (1960); A. Blandin and J. Friedel, Phys. Chem. Solids **17**, 170 (1960); A. Blandin, J. Phys. Radium **22**, 507 (1961).
[7] W. Kohn and S. H. Vosko, Phys. Rev. **119**, 912 (1960). J. S. Langer and S. H. Vosko, Phys. Chem. Solids **12**, 196 (1959).
[8] P. L. Sagalyn, A. Paskin, and R. J. Harrison, Phys. Rev. **124**, 428 (1961).
[9] R. M. Steffen, Phys. Rev. **103**, 116 (1956).
[10] G. Hinman, G. R. Hoy, J. K. Lees, and J. C. Serro, following paper, Phys. Rev. **135**, A218 (1964).

TABLE I. Summary of experimental results.

Z'_0	Solute	Concentration in atomic%	$\hat{G}_2$[a]	Concentration from chemical analysis in atomic%	Concentration from residual resistivity in atomic%	Oxygen Concentration in atomic%
0	Cu	0.46	0.78±0.03	0.46		
0	Cu	0.62	0.74±0.02	0.62		
0	Cu	1.28	0.55±0.01	1.28		
0	Au	0.27	0.90±0.02	0.26	0.28	
0	Au	0.46	0.84±0.01	0.42	0.50	0.017
0	Au	0.80	0.69±0.02	0.78	0.81	
0	Au	1.17	0.70±0.04	1.17		
1	Zn	0.53	0.86±0.01	0.53		
1	Zn	0.79	0.89±0.01	0.83	0.75	0.003
1	Zn	0.82	0.87±0.02	0.81	0.83	
1	Cd[b]	0.50	0.83±0.03	0.50		
2	Al	0.25	0.90±0.04	0.20	0.29	0.038
2	In[b]	0.44	0.71±0.02	0.45	0.42	
2	Tl	0.48	0.66±0.02	0.51	0.44	0.006
2	Tl	0.30	0.78±0.03	0.31	0.30	0.014
3	Ge[b]	0.25	0.84±0.02	0.25		
3	Ge[b]	0.49	0.69±0.02	0.49		
3	Ge[b]	0.62	0.62±0.01	0.62		
3	Sn[b]	0.45	0.63±0.02	0.52	0.38	
3	Pb	0.31	0.75±0.02	0.30	0.32	0.015
3	Pb	0.33±0.13	0.71±0.02	0.45	0.20	0.15
3	Pb	0.75	0.52±0.02	0.67	0.84±0.06	
4	As	0.29	0.71±0.01	0.29	0.29	0.0007
4	As	0.57	0.51±0.02	0.62	0.52	0.01
4	Sb	0.25	0.70±0.01			
4	Sb[b]	0.51	0.53±0.03	0.51		
4	Sb	1.0	0.28±0.03			

[a] The values listed here are actually ratios of $\hat{G}_2$ for the alloys to the average $\hat{G}_2$ for our pure silver samples.
[b] Taken from Ref. 3.

(1) an attenuation factor[11] $G_k(t)$ which depends on the strength of the interaction and on the time t for which the perturbation acts before the intermediate state decays. This factor is treated in more detail in Sec. IV. The experiment measures a double average of $G_2(t)$ designated as $\hat{G}_2$. The first average is taken over the sensitive period of the coincidence circuit which records the coincidence counting rate, with weighting proportional to the decay rate e^{-t/τ_n} of the intermediate state. Here τ_n is the mean life of the intermediate state. The second average is made over all possible interaction strengths (determined by the relative positions of solute and probe ions), each weighted by its probability of occurrence. In the calculation of the latter weight factors it is assumed that the solute and probe ions are situated at random in the lattice. This assumption is considered in detail in Appendix I.

In addition to the averaging described above, the measured correlation also includes the effect of the finite angular resolution of the detectors. For cylindrically symmetric detectors it can be shown[12] that this introduces a geometrical factor b_k into each term of Eq. (1). The final expression for the measured correlation function in this experiment is

$$W_E(\vartheta)=1+A_2b_2\hat{G}_2P_2(\cos\vartheta), \qquad (2)$$

where ϑ is now the angle subtended at the source by the axes of the detectors. In this experiment, the value of the factor $A_2b_2\hat{G}_2$ is extracted from the ratio of the coincidence counting rates measured at 90° and 180°. For each alloy $\hat{G}_2$ is then obtained by dividing the measured value of the factor $A_2b_2\hat{G}_2$ by the experimental value of A_2b_2, which is obtained from identical measurements on pure silver for which it is assumed that $\hat{G}_2=1$ (no attenuation). This assumption is shown in the following paper[10] to be satisfactory.

The samples in these experiments are all silver alloys. They contain three components, namely Ag, solute, and In^{111} in the approximate atomic ratios of 1 Ag, 0.005 solute, and 10^{-9} In^{111}. The samples are disks 7/32-in. in diameter and 0.014 in. thick. They have been annealed in an evacuated tube for 24 h at 890°C just before being measured. X-ray analysis shows them to be polycrystalline with randomly oriented grains. The grain size varies from 10 to 30 μ.

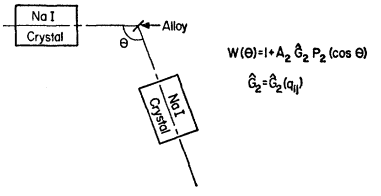

FIG. 2. Counter arrangement for angular correlation measurements.

[11] A. Abragam and R. V. Pound, Phys. Rev. **92**, 943 (1953).
[12] M. E. Rose, Phys. Rev. **91**, 610 (1953).

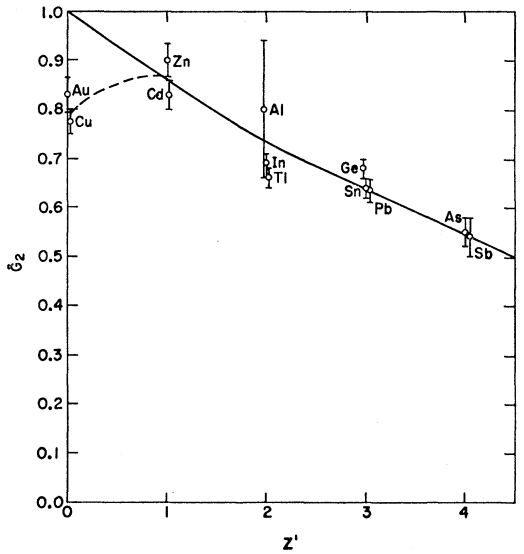

FIG. 3. Correlation of angular correlation data with solute valence.

The experimental equipment and procedures used in this work have been previously described.[3] Summarizing briefly the apparatus consists of two counters arranged as shown in Fig. 2. The electronics is designed to count delayed coincidences between two gamma rays coming from the source. A coincidence is recorded if γ_2 is detected between 155 nsec and 335 nsec after γ_2. The data are automatically recorded and converted to values for $\hat{G}_2$. Recently the automatic camera used to record scaler counts in earlier work was replaced by a system which records the accumulated scaler counts on punched paper tape.

Preparation of the alloys has also been described in detail in Ref. 3. The present procedure is the same except that the alloy billets are now given an additional anneal for 24 h to improve homogeneity. The annealing temperature has usually been 890°C, although 790°C was used for Pb and As. The composition of each alloy was determined by chemical analysis, using several portions of the billet or rolled specimens, and also by residual resistivity measurements. The silver used was in most cases 99.999% pure, although a few measurements have been made with 99.99% pure material. The solute materials were at least 99.99% except for Tl which was 99.98% and Au which was 99.9% pure. A number of the alloys were analyzed for oxygen by the vacuum fusion technique. The possible effects of any impurities present in the alloys are discussed in the Appendix.

The results of these analyses are given in Table I, together with the experimental attenuation factors for all of the alloys studied. Each $\hat{G}_2$ quoted represents the average of a number of individual disks, usually four or five. The concentration listed in column two is the best value based on all sample analyses carried out. For the 0.25% Sb and the 1.0% Sb no analyses were done and the values are determined by the weights of the constituent materials used in making the billets. The concentration in column six is found from the resistivity measured for the alloy and the published value of residual resistivity per atomic percent of solute.[13]

In order to display the experimental results more clearly, curves have been drawn of $\hat{G}_2$ versus solute concentration and the value of $\hat{G}_2$ at 0.50% impurity concentration determined. In the case of a solute for which only one concentration was measured, the curve was based on the measured point and the point $\hat{G}_2=1$ for pure silver. In Fig. 3 these values of $\hat{G}_2$ at 0.5% are plotted as a function of Z', the valence difference between the solute and silver. The correlation is quite good except for the deviations at $Z'=0$. To show that the value of $\hat{G}_2$ is not very well correlated with a size parameter alone the $\hat{G}_2$ values at 0.5% were plotted in Fig. 4 against $(1/a)(da/dc)$, the rate of change of lattice parameter with solute concentration. Here the correlation is poor. It is interesting to compare these curves with the series done on Cu alloys by Rowland. In Figs. 5 and 6 the "wipe out" numbers of Rowland,[2] essentially the number of Cu sites around a solute at which the field gradient exceeds a critical size, are plotted as a function of Z' and $(1/a)(da/dc)$, respectively. The features are very similar with the same deviations at $Z'=0$ in Fig. 4 and the general lack of correlation with the size parameter.

III. THEORETICAL MODEL

The field-gradient components at a probe nucleus, $q_{ij}=\partial^2 V/\partial x_i \partial x_j - \frac{1}{3}\delta_{ij}\nabla^2 V$, can be obtained by differentiating the electrostatic potential V produced at the

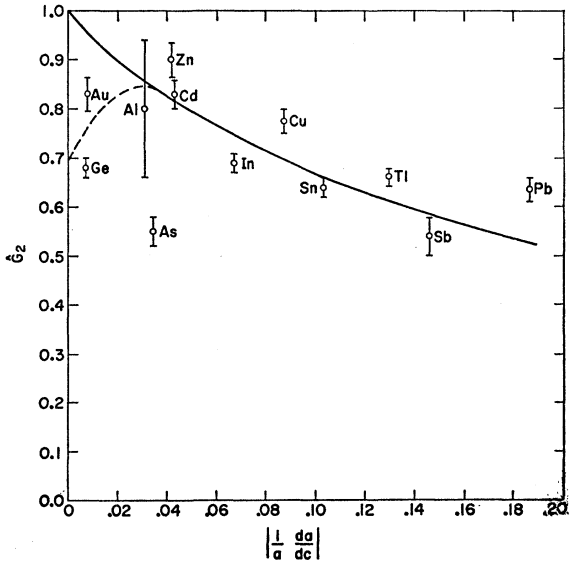

FIG. 4. Correlation of angular correlation data with change in lattice parameters.

[13] A. N. Gerritsen, in *Handbuch der Physik*, edited by S. Flügge (Springer-Verlag, Berlin, 1956), Vol. 19, p. 206.

nucleus by the charge distribution around it. This charge distribution can be written as the sum of two terms. One is the conduction electron charge. The other is the charge produced by the rest of the electrons and by the nuclei of the atoms in the lattice. Calling these, respectively, $\rho_1(r)$ and $\rho_2(r)$,

$$V(\mathbf{r})=\int \frac{\rho_1(\mathbf{r}')d^3r'}{|\mathbf{r}-\mathbf{r}'|}+\int \frac{\rho_2(\mathbf{r}')d^3r'}{|\mathbf{r}-\mathbf{r}'|}. \tag{3}$$

In the absence of a perturbation of the lattice near the probe, the field-gradient components should vanish because of the cubic symmetry with respect to the probe site. The presence of a solute atom near the probe removes this symmetry, and field gradients are produced at the probe. The contributions to the field gradient have been discussed by a number of investigators.[5–8] The principal component comes from scattering of the conduction electrons by the solute atom. The perturbed electron density is not well known within the solute ion itself, but for the region outside the solute approximate treatments have been given. Actually, two centers of perturbation are present in the experiments reported here. The probe itself is one, but because cubic symmetry is maintained with respect to the probe nucleus, the field gradient components are zero unless a solute ion is nearby. The perturbing electron density can be expressed as

$$\Delta n(\mathbf{r})=\frac{2}{(2\pi)^3}\int \Delta n_{\mathbf{k}}(\mathbf{r})d^3k, \tag{4}$$

where

$$\Delta n_{\mathbf{k}}(\mathbf{r})=|\Psi_{\mathbf{k}}(\mathbf{r})|^2-|\Psi_{0\mathbf{k}}(\mathbf{r})|^2. \tag{5}$$

In these expressions $\Psi_{\mathbf{k}}(\mathbf{r})$ is the Bloch wave function

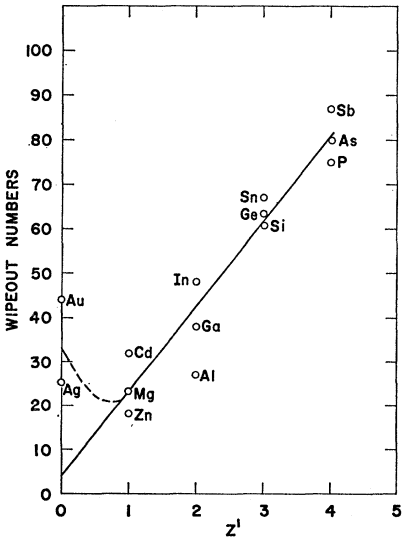

FIG. 5. Correlation of Rowland's data with solute valence. Data taken from T. J. Rowland, Phys. Rev. **119**, 900 (1960).

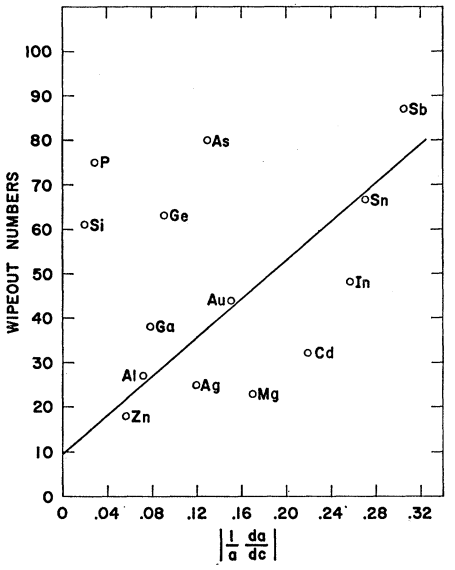

FIG. 6. Correlation of Rowland's data with change in lattice parameter. Data taken from T. J. Rowland, Phys. Rev. **119**, 900 (1960).

with wave vector $\mathbf{k}$ for an electron in the vicinity of both a solute ion and a probe ion and $\Psi_{0\mathbf{k}}(\mathbf{r})$ is the corresponding wave function when only the probe ion is present. If the wave function $\Psi_{\mathbf{k}}(\mathbf{r})$ is written

$$\Psi_{\mathbf{k}}(\mathbf{r})=\Psi_{0\mathbf{k}}(\mathbf{r})+v(\mathbf{r}), \tag{6}$$

then to first order in $v(\mathbf{r})$

$$\Delta n_{\mathbf{k}}(\mathbf{r})=\Psi_{0\mathbf{k}}{}^*(\mathbf{r})v(\mathbf{r})+\Psi_{0\mathbf{k}}(\mathbf{r})v^*(\mathbf{r}). \tag{7}$$

The wave function $\Psi_{0\mathbf{k}}(\mathbf{r})$ is approximated by $\phi_{\mathbf{k}}(\mathbf{r})$, the wave function for a pure silver lattice, in the further developments in this paper. Partial experimental justification of this replacement can be found in the experiments of Drain[14] on the Knight shift in Cd-Ag alloys. He showed that the conduction-electron wave function is not very different at the cadmium sites and the silver sites. With this approximation the $\Delta n_{\mathbf{k}}(\mathbf{r})=\phi_{\mathbf{k}}{}^*(\mathbf{r})v(\mathbf{r})+\phi_{\mathbf{k}}(\mathbf{r})v^*(\mathbf{r})$. This reduces to the case treated by Kohn and Vosko[7] if the probe atom is ignored in evaluating $v(\mathbf{r})$. Flynn[15] has discussed this assumption and has shown that it is a good approximation. It will be used in the rest of this paper.

Kohn and Vosko have derived the leading term in an asymptotic series for q_{ij}.[7] They assume that the Fermi surface is spherical, a good but not perfect assumption for silver. This means that the electric-field-gradient tensor at the probe nucleus will have axial symmetry with respect to an axis running from the solute nucleus out through the probe. Calling this the z' axis and choos-

[14] L. E. Drain, Phil. Mag. **4**, 484 (1959).
[15] C. P. Flynn, Phys. Rev. **126**, 533 (1962).

ing the x' and y' axes to complete a triad,

$$\begin{aligned} &q_{z'z'}{}^{v}=eq', \quad (e \text{ is the magnitude of the electronic charge})\\ &q_{x'x'}{}^{v}=q_{y'y'}{}^{v}=-\tfrac{1}{2}eq', \\ &q_{ij}{}^{v}=0 \quad i\neq j, \end{aligned} \tag{8}$$

where $q'=(8\pi/3)\alpha A\cos(2k_0r+\phi)/3$. The origin of $\mathbf{r}$ is at the solute ion. The wave number k_0 is the value at the Fermi surface. The constants A and ϕ can be expressed in terms[7] of the phase shifts for electron scattering.

$$A=\frac{1}{2\pi^2}\{[\sum_l(2l+1)\{-\sin\eta_l\cos(\eta_l-l\pi)\}]^2 +[\sum_l(2l+1)\{-\sin\eta_l\sin(\eta_l-l\pi)\}]^2\}^{1/2}, \tag{9}$$

$$\phi=\tan^{-1}\left\{\frac{-\sum_l(2l+1)\sin\eta_l\sin(\eta_l-l\pi)}{-\sum_l(2l+1)\sin\eta_l\cos(\eta_l-l\pi)}\right\}.$$

The factor α is an enhancement factor estimated[3] to be about 57 for silver.

The second term in (3) represents the effects other than those produced by the conduction-electron scattering at the solute and the consequent core polarization at the probe. This field gradient is very difficult to calculate and includes a number of more or less separable components. One of these is the gradient coming from the silver ions as a result of their displacement by the solute. When these ions move from their equilibrium positions, cubic symmetry with respect to the probe is destroyed and a field gradient will exist at this point. On the other hand, this perturbing effect of the distorted lattice on the probe will be partially shielded out by the conduction electrons. If one neglects the induced polarization of the probe cores, the residual effect for each silver ion will be somewhat like that for a shielded dipole. The field gradient resulting the polarization of the probe core, however, is probably the dominant one because of the proximity of the core to the probe nucleus. Its magnitude will depend on the extent of the overlap of the silver cores with the probe core and hence on the displacement of the probe ion with respect to its nearest neighbors. A final contribution to the field gradient comes from the conduction-electron rearrangement around the probe as a result of its displacement by the solute.

In this paper it will be assumed that the principal contribution to the field-gradient tensor at the probe nucleus comes from the effects of overlap of the core electrons of the probe with those of the nearest-neighbor silver atoms, twelve in number. This field gradient is proportional, through an enhancement factor, to the field gradient which would be produced at the probe directly by the core electrons of the nearest silver ions. These core electrons are almost spherically symmetric about their respective ion centers, so that the symmetry of the field-gradient tensor should be correctly given by calculating it as though it came from point charges located at the centers of the twelve nearest neighbors to the probe as displaced by the solute. This value is then multiplied by a constant λ adjusted to give a best fit to experiment. This constant includes the effects of the enhancement factor and the difference between the effective charge of the core electrons and a unit positive charge. The displacements produced by the probe are not included because they have cubic symmetry with respect to the probe nucleus and hence do not produce a field gradient there.

According to the model described above, the field gradient produced by the second term in Eq. (3) can be written

$$q_{jk}{}^{s}=\lambda\partial^2V_s/\partial x_j\partial x_k \tag{10}$$

where

$$V_s=e\sum_i\left(\frac{1}{|\mathbf{r}_{ip}|}-\frac{1}{|\mathbf{a}_{ip}|}\right) \tag{11}$$

and e is a positive number. In this equation the $\mathbf{r}_{ip}$ is the vector from the probe ion to the ith neighboring silver ion with both displaced by the solute ion and $\mathbf{a}_{ip}$ is the corresponding vector with no displacement. The summation is carried out over the twelve nearest neighbors to the probe ion. The $q_{jk}{}^{s}$ has been evaluated to terms linear in the displacements.

$$q_{jk}{}^{s}=3\lambda e\sum_i\left\{\delta_{jk}\frac{\mathbf{a}_{ip}\cdot\boldsymbol{\varrho}_{ip}}{a_{ip}{}^5}-\frac{5}{a_{ip}{}^5}\frac{a_{ip}{}^{(j)}}{a_{ip}}\frac{a_{ip}{}^{(k)}}{a_{ip}}(\mathbf{a}_{ip}\cdot\boldsymbol{\varrho}_{ip}) +\frac{1}{a_{ip}{}^5}(\rho_{ip}{}^{(j)}a_{ip}{}^{(k)}+a_{ip}{}^{(j)}\rho_{ip}{}^{(k)})\right\}, \tag{12}$$

where $\boldsymbol{\varrho}_{ip}=\mathbf{u}_i-\mathbf{u}_p$. $\mathbf{u}_i$ is the displacement of the ith silver ion by the solute and $\mathbf{u}_p$ is the displacement of the probe ion by the solute. A superscript in parentheses denotes a component of a vector quantity.

This field gradient is more complicated than the one used by Sagalyn, Paskin, and Harrison[8] in their analysis of the experiments of Rowland. It does not have axial symmetry and this fact makes the evaluation of the attenuation factor for the angular correlation more difficult. Analysis of most of the present data in terms of the method of Sagalyn *et al.* is given in Hinman, Hoy, and Lees.[3]

In order to calculate $q_{jk}{}^{s}$ it is necessary to know the displacements of silver ions around a solute. There does not appear to be very much information available on this subject. There are a number of calculations of the relaxation of lattices near vacancies from which it appears that the displacement depends strongly on direction. Presumably this will also be true for the displacement near a solute. However, in the absence of better information the usual displacement field for an isotropic elastic medium[8] has been used in this paper,

TABLE II. Input data for G_2 calculations.

Solute	Z_0'	Residual[a] resistivity per atomic%	Z'[b]	A	ϕ	η_0	η_1	$(1/a)(da/dc)$[c]
Au	0	0.36	0.018	0.02030	3.2283	0.218	−0.063	−0.00819
Cu	0	0.077	0.185	0.0095	3.7119	0.165	0.043	−0.0871
Cd	1	0.382	0.889	0.02463	0.1770	0.460	0.312	0.043
Zn	1	0.64	1.093	0.03078	0.2280	0.563	0.385	−0.0417
Al	2	1.95	1.931	0.0459	−0.2327	2.591	0.148	−0.031
In	2	1.78	1.826	0.0409	−0.3380	2.563	0.102	0.067
Tl	2	2.27	1.713	0.04355	−0.4921	2.427	0.088	0.1295
Ge	3	5.5	2.978	0.0973	0.4900	2.840	0.613	0.0071
Pb	3	4.65	2.584	0.08507	0.2356	2.645	0.472	0.187
Sn	3	4.36	2.760	0.0856	0.3653	2.814	0.507	0.093
As	4	8.5	3.918	0.1237	1.0032	3.218	0.979	0.0347
Sb	4	7.25	3.666	0.1143	0.8721	3.173	0.862	0.146

[a] Values taken from Ref. 13.
[b] Calculated by prescription of Blatt, Ref. 17.
[c] Values taken from E. A. Owen and V. W. Rowlands, J. Inst. Metals **66**, 361 (1940), except for Ge, distortion parameter for Ge taken from W. Hume-Rothery, G. F. Lewin, and P. W. Reynolds, Proc. Roy. Soc. (London) **A157**, 167 (1963).

i.e., $\mathbf{u}=(3a^3/16\pi\gamma_E)[(1/a)(da/dc)](\mathbf{r}/r^3)$, where a is the lattice parameter, da/dc is its change with solute connection, $\gamma_E=3(1-\sigma)/(1+\sigma)$, σ is Poisson's ratio, and $\mathbf{r}$ is the distance from the center of the solute ion to the center of the ion whose displacement is $\mathbf{u}$. This will at least give a good estimate of the "average" displacement because the lattice parameter changes which determine $(1/a)(da/dc)$ depend on contributions from many ions around each solute.

IV. APPLICATION TO EXPERIMENT

The attenuation of the angular correlation to be expected in the case where the nuclei are in an electric field gradient without axial symmetry is tedious to calculate.

For the case of the interaction in the intermediate state of the quadrupole moment of the Cd^{111} nucleus with the electric field gradient, the expression for the attenuation factor is[10]

$$G_k(t)=\frac{1}{2I+1}\sum_{\mu mm',bb'}(Ikm\mu|IkIm+\mu)\times(Ikm'\mu|IkIm'+\mu)\times(m+\mu|b)(b|m'+\mu)\times(m'|b')(b'|m)\cos\omega_{bb'}t. \quad (13)$$

In this expression t is the time interval between the emissions of the first and second gamma rays; I is the intermediate state spin, $\frac{5}{2}$ in this case; the appropriate value of k here is 2; m and μ are the magnetic quantum numbers associated with spins I and k, respectively, referred to a quantization axis which coincides with the z direction in the principal axis system of the field-gradient tensor; $|b)$ and E_b are the corresponding eigenstates and eigenvalues of the quadrupole interaction Hamiltonian;[16] and $\omega_{bb'}=(E_b-E_{b'})/\hbar$. The nonvanishing elements of the quadrupole interaction Hamiltonian using the principal axes are

$$\begin{aligned}&\langle m|\mathcal{H}|m\rangle=A[3m^2-I(I+1)]V_0,\\&\langle m\pm2|\mathcal{H}|m\rangle=A[(I\mp m)(I\mp m-1)\times(I\pm m+1)(I\pm m+2)]^{1/2}V_2,\\&V_0=q_{zz}{}^v+q_{zz}{}^s;\quad V_2=\tfrac{1}{2}(q_{xx}{}^v+q_{xx}{}^s-q_{yy}{}^v-q_{yy}{}^s);\\&A=\frac{eQ}{4I(2I-1)}.\end{aligned} \quad (14)$$

The expression (13) is difficult to evaluate because the field gradient calculated in Sec. III does not have axial symmetry. Thus, the Hamiltonian is not diagonal in the representation consisting of the set of states $|m)$. The evaluation of $G_2(t)$ has been carried out using the Bendix G20 computer at Carnegie Institute of Technology. For each solute-probe configuration the program computes the total field-gradient tensor

$$q_{jk}{}^t=q_{jk}{}^v+q_{jk}{}^s \quad (14)$$

given by the sum of Eqs. (8) and (12), and locates its principal axes. Then it calculates the matrix elements of the interaction Hamiltonain in the principal axis frame of reference, diagonalizes the matrix to find its eigenstates and eigenvalues, and performs the sums indicated in Eq. (13) to obtain the value of $G_2(t)$ for the given probe-solute configuration. This result is then averaged over the sensitive period of the coincidence circuit, which, as mentioned previously, accepts coincidences if t lies between $t_1=155$ nsec and $t_2=335$ nsec (nsec$\equiv10^{-9}$ sec). Therefore, the time-averaged value $\bar{G}_2$ must be computed, involving

$$\langle\cos\omega_{bb'}t\rangle_{\rm av}=\int_{t_1}^{t_2}e^{-t/\tau n}\cos\omega_{bb'}t\,dt\Big/\int_{t_1}^{t_2}e^{-t/\tau n}dt. \quad (15)$$

The final result $\hat{G}_2$ for comparison with experiment is obtained by averaging $\bar{G}_2$ over all possible solute-probe configurations, as noted in Sec. II. In the evaluation of

[16] M. H. Cohen and F. Reif, in *Solid State Physics*, edited by F. Seitz and D. Turnbull (Academic Press Inc., New York, 1957), Vol. 5.

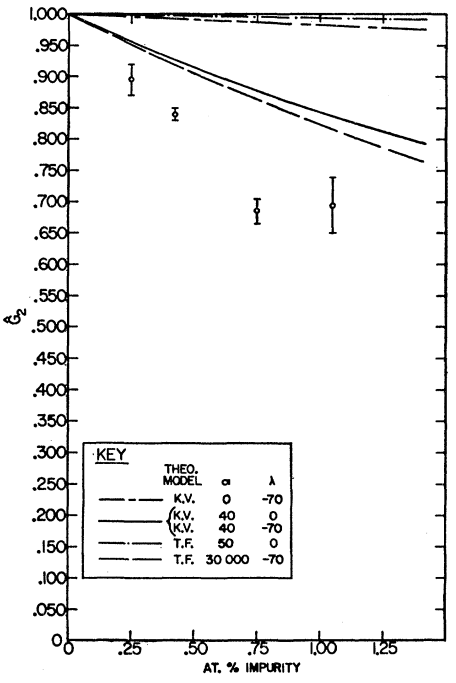

FIG. 7. Comparison of experiments with calculations for Au.

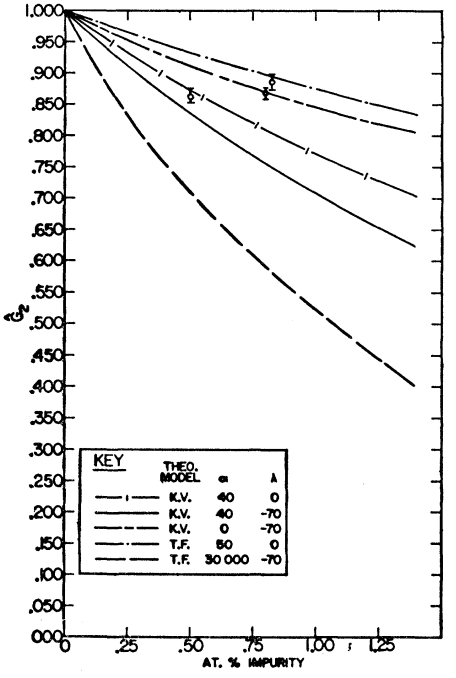

FIG. 9. Comparison of experiments with calculations for Zn.

Eq. (13) it is assumed that the field gradient (14) at the probe nucleus is due to the nearest solute ion only. With the dilute concentrations used in these experiments it is very improbable that there will be another solute at approximately the same distance. Designating by P_i the probability that the solute ion nearest to the probe is in the ith neighbor position, and by $(\bar{G}_2)_i$ the time-averaged attenuation factor for that configuration, we have finally

$$\hat{G}_2=\sum_i P_i(\bar{G}_2)_i. \tag{16}$$

The information about each solute required to cal-

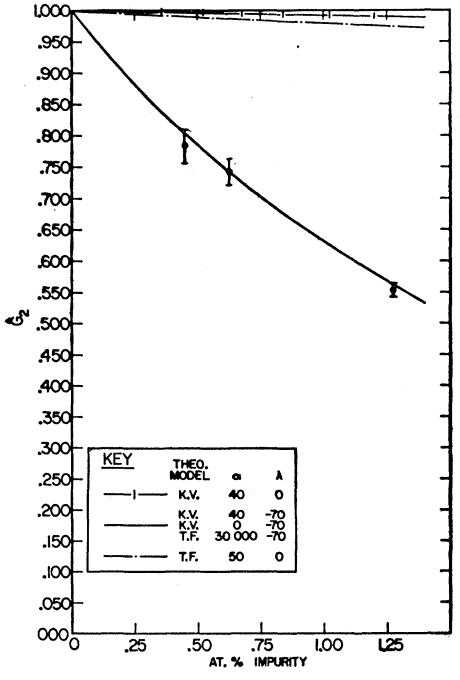

FIG. 8. Comparison of experiments with calculations for Cu.

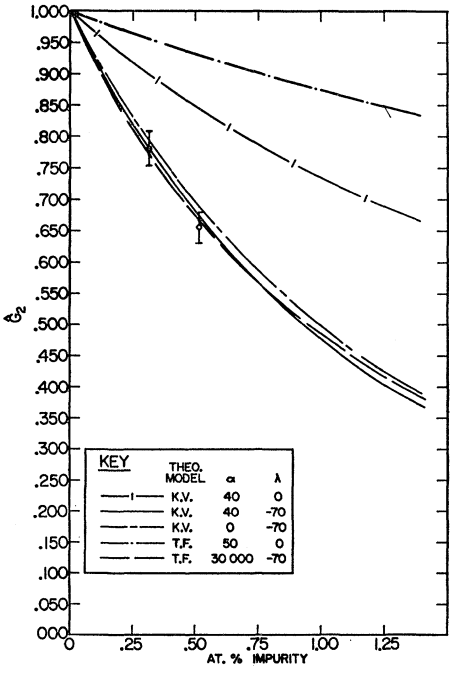

FIG. 10. Comparison of experiments with calculations for Tl.

TABLE III. Comparison of calculation with esperiment.

Impurity	$\hat{G}_2$ ½% Exp. Val.	(Theoretical values of $\hat{G}_2$ at ½ at.%) K.V. $\hat{G}_2$ α λ 40, 0	K.V. $\hat{G}_2$ α λ 40, −70	K.V. $\hat{G}_2$ α λ 0, −70	T.F. $\hat{G}_2$ α λ 50, 0	T.F. $\hat{G}_2$ α λ 30 000, −70
Au	0.83±0.04	0.913	0.911	0.991	0.995	0.905
Cu	0.78±0.03	0.995	0.779	0.780	0.989	0.777
Cd[a]	0.83±0.03	0.897	0.878	0.907	0.938	0.727
Zn	0.90±0.04	0.869	0.832	0.911	0.934	0.706
Al[a]	0.80±0.14	0.821	0.821	0.942	0.934	0.697
In[a]	0.69±0.02	0.844	0.765	0.835	0.934	0.684
Tl	0.66±0.02	0.847	0.673	0.692	0.934	0.668
Ge	0.68±0.02	0.674	0.672	0.992	0.935	0.665
Pb	0.64±0.03	0.700	0.589	0.630	0.931	0.612
Sn[a]	0.64±0.02	0.693	0.638	0.765	0.932	0.655
As	0.55±0.03	0.649	0.616	0.932	0.938	0.655
Sb	0.54±0.04	0.643	0.576	0.669	0.939	0.614

[a] There is only one experimental value for each of these impurities.

culate $\hat{G}_2$ includes the phase shifts η_l and the value of $(1/a)(da/dc)$. To find the phase shifts the semiempirical method of Kohn and Vosko[7] has been used. In this method the shifts for $l>1$ are taken to be zero. The values of η_0 and η_1 are found from the Friedel sum rule[6] $Z'=(2/\pi)\sum_l(2l+1)\eta_l$ and the residual resistivity, $\Delta\rho=(4\pi c\hbar/e^2k_0)\sum_l l\sin^2(\eta_{l-1}-\eta_l)$. The uniqueness of these phase shifts is further discussed in Appendix II. The values of Z' used are not integers but have been altered according to the prescription of Blatt[17] to take account of the variation of the positive charge in the region of the solute. In Table II is a summary of the data used, the phase shifts, and the A and ϕ values for the solutes studied. A and ϕ give the perturbed electron density in the free electron approximation, $\Delta n_{\text{free}}=A[\cos(2k_0r+\phi)/r^3]$.

The quantities αQ and λQ, which appear as factors multiplying the valence and size terms, respectively, in the quadrupole Hamiltonian, are used as adjustable parameters to fit the data. The quadrupole moment Q of the excited state of Cd^{111} is taken to be 10^{-24} cm^2. The value for this moment has been discussed previously[3] and 10^{-24} cm^2 is perhaps somewhat high. It is subject to considerable uncertainty because of the limited accuracy with which the field gradient is known in the experiments where the quadrupole interaction has been measured. Another value of Q can be substituted if α and λ are also modified to maintain the same optimum values of αQ and λQ. It would be difficult, however, to explain the large values of α and λ that would be required to explain the present experiments if Q is as small as the 0.15×10^{-24} cm^2 proposed by Das and Pomerantz.[18]

V. DISCUSSION OF RESULTS

The experimental results for eight of the solutes are shown in Figs. 7–14 together with a number of calculated curves. The curves labeled K.V. are calculated by using the Kohn Vosko screening of the solutes by the conduction electrons and the model for the strain calculation described in the preceding section of this paper. The curves labeled T.F. (Thomas-Fermi) are calculated by using the exponential shielding potential $(Z'e/r)e^{-r/a}$ with $a=0.586\times10^{-8}$ cm. Using the Kohn Vosko model the value $\alpha=40$ was selected to match the data for Ge. This solute was chosen for the determination of α because it distorts the silver lattice very little and the size effect should be small. Thus, the calculated value of $\hat{G}_2$ is very insensitive to the value of λ for Ge. On the other hand, the valence effect alone gives very poor agreement with the experimental attenuation for Cu. The field gradient produced by a Cu ion would have to be large enough to cause "hard core" attenuation of 0.2 out to and including third neighbors in order to explain the observed $\hat{G}_2$, if only the valence effect were present. This should be beyond the range of large deviations from the asymptotic form of Kohn and Vosko. The Cu attenuation was therefore used to evaluate the size parameter λ, which was found to have the value $\lambda=-70$. The negative sign for λ is to be expected according to the model in this paper because the field gradient is considered to be produced by electrons, and the potential with $\lambda=1$ has the proper sign for positive charges. The large magnitude of λ is disturbing. According to the present model the perturbers are the $4d$ electrons of which there are ten. Thus, the perturbation could be considered to come from these ten electrons each with an enhancement factor of 7. This possibility has not been investigated quantitatively, and $\lambda=-70$ is accepted as an empirical parameter.

The rest of the curves, taking $\alpha=40$ and $\lambda=-70$, give reasonably good agreement with the experimental points except those for Zn and Au. On the other hand, there are a number of solutes (Cu, Tl, Pb, Sb) for which the curves without the size effect ($\alpha=40$, $\lambda=0$) differ markedly from the experimental points. The size term somewhat improves agreement with experiment.

The data are presented in Table III for all twelve

[17] F. J. Blatt, Phys. Rev. **108**, 285 (1957).
[18] M. Pomerantz and T. P. Das, Phys. Rev. **119**, 70 (1960).

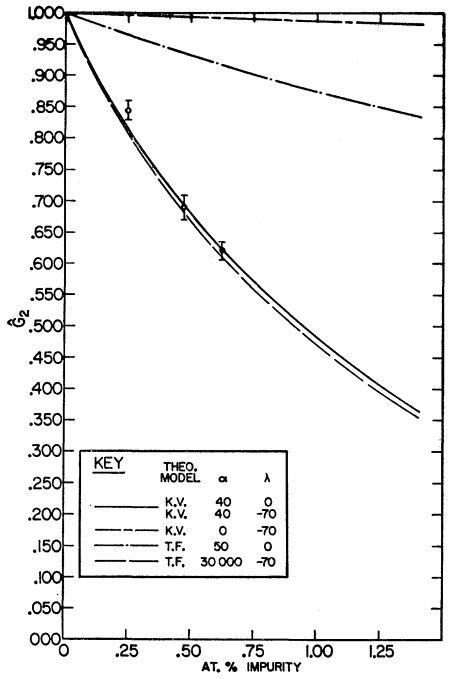

FIG. 11. Comparison of experiments with calculations for Ge.

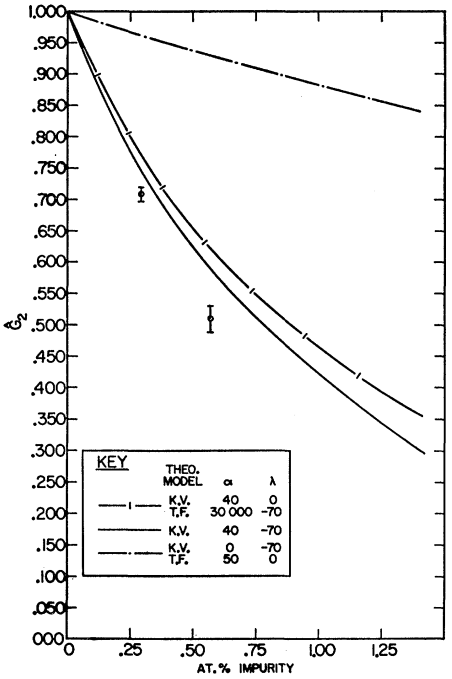

FIG. 13. Comparison of experiments with calculations for As.

solutes in the series at 0.5% solute concentration. The experimental values at 0.5% are taken from the best curves drawn through the actual data. In the case of a solute for which only one concentration was measured, this one point and the point $\hat{G}_2=1$ at zero impurity concentration were used to draw the curve. The calculated values are based either on the long-range shielding (K.V.) or the Thomas-Fermi shielding (T.F.). There is improved agreement between experiment and calculation in a number of cases (Cu, In, Tl, Sn, Sb) when the size term is included.

The figures and tables also show the shortcomings of

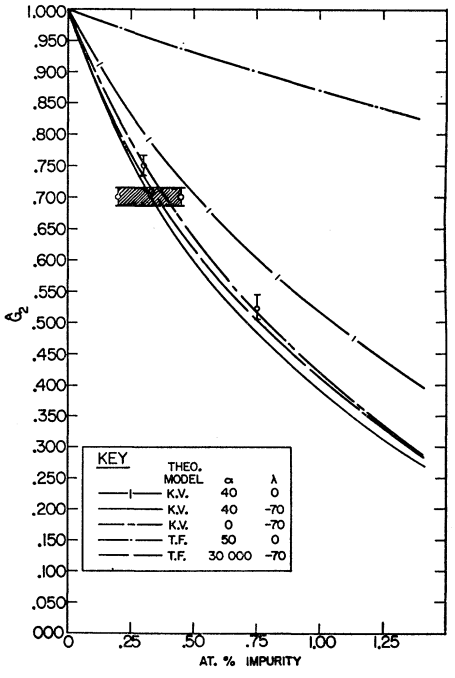

FIG. 12. Comparison of experiments with calculations for Pb.

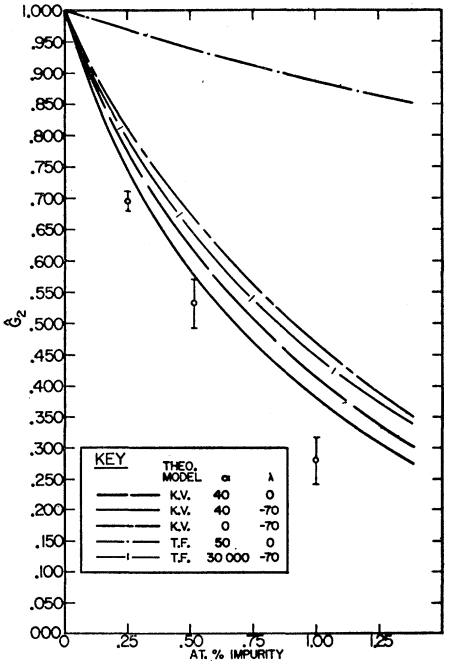

FIG. 14. Comparison of experiments with calculations for Sb.

Thomas-Fermi screening. With a reasonable value of $\alpha(\alpha=50)$ the valence term contributes a negligible amount to the attenuation. In order to account for the Ge result using Thomas-Fermi screening it is necessary to give α the enormous value of 30 000. Even with this latter α the agreement is poor with a number of solutes (Cd, Zn, As, Sb). These results can easily be understood qualitatively for the Thomas-Fermi shape potential in view of the rapid variation of q_{ij} with distance from the solute.

One advantage of the present calculation of the size effect in comparison to the model used in the second paper of Ref. 3 is that it eliminates the necessity for adding absolute values.

VI. CONCLUSIONS

In summary these experiments and calculations indicate the following:

(1) $\hat{G}_2$ is well correlated with Z' and poorly correlated with $(1/a)(da/dc)$.

(2) Nevertheless, agreement between calculation and experiment is somewhat improved by including a size or strain term. It does not seem possible to explain the results for Cu or Tl on the basis of the valence term alone.

(3) There remains an unresolved discrepancy for Zn and Au that may be an effect of probe-solute association.

(4) The Thomas-Fermi shielding is inconsistent with experiment.

ACKNOWLEDGMENTS

The authors would like to thank Robert Kribel for assistance in taking data during part of these experiments.

The Lewis Research Center of the National Aeronautics and Space Administration and the Argonne National Laboratory kindly performed the many α-particle bombardments.

APPENDIX I: DISCUSSION OF EXPERIMENTAL PROBLEMS

Possible experimental difficulties with this technique have been discussed in Ref. 3 and somewhat more generally in Ref. 19. They include recoil effects from the K capture preceding the gamma cascade and from the first gamma emission itself. They also include perturbing effects of dislocations and impurities in the silver. Impurities are to be distinguished from the solutes deliberately introduced.

Measurements in the case of pure silver as reported in Ref. 3 and the succeeding paper in this journal show that the angular correlation is very little attenuated. Therefore, recoil effects are presumably not important in these experiments (however, see the discussion by Steffen[9] on this point), and impurities in the pure silver do not cause trouble.

Turning to the measurements on the alloys there are a number of effects of concern. One is association of the probes with minority impurities. The other is association of the probes with the solutes. Association with minority impurities will produce spurious attenuation of the correlation. However, there are several reasons for discounting this possibility. The impurity concentration contributed by the addition of a small amount of solute to the silver is negligible compared to the impurity concentration present in the silver itself. Therefore the fact that the correlation in pure silver is very little attenuated indicates that minority impurities should be unimportant. Furthermore, there is a large entropy of mixing associated with these impurities. At the annealing temperature of 890°C, presumably the temperature that determines the equilibrium conditions in the samples, an association energy of about 1 eV is required to produce appreciable association of the probes with an impurity present to 1 part in 10^6. This is considerably larger than estimates of association energies expected in metals. A third reason for discounting impurity-probe association is that in most cases an impurity that will associate with an In ion will also associate with the solute ions present. The result will be that most impurities will in such cases be on solute ions rather than probe ions. A final reason for discounting effects of minor impurities is the observed variation of $\hat{G}_2$ with the concentration of solute. Such a variation would not be expected if most of the attenuation was caused by impurity ions.

On the other hand, association of the probes with solutes may be present. Here the concentration is of the order of 0.5 at.% solute. An association energy of 0.25 eV, provided that it is attractive, should be enough to appreciably alter probe-solute distribution and affect the attenuation of the correlation. Blandin and DePlante[5] have estimated solute interactions in metals. From their work it appears that two solute ions with the same sign of Z' should repel each other in the first neighbor position. Furthermore, the magnitude of the interaction energy in the second and more distant neighbor positions seems to be below the value required for appreciable association at 890°C. However, additional experiments are in progress to check the possibility of association effects; they involve variations of the heat treatment given to specimens before measurements are made.

There is a possibility that the probe ions and the solute ions may collect around dislocations so that the attenuation factor $\hat{G}_2$ would be lowered. Presumably solute ions are attracted to dislocation lines whether they are larger or smaller than the ions of the matrix.[20] There are a number of reasons for believing that this effect is not important. In the first place, a probe nucleus should be in an appreciable field gradient at a

[19] E. Heer and T. Novey, *Solid State Physics*, edited by F. Seitz and D. Turnbull (Academic Press Inc., New York, 1959), Vol. 9.

[20] A. Granato and K. Lucke, J. Appl. Phys. **27**, 789 (1956).

dislocation if there is enough interaction to cause it to migrate there, but the angular correlation is almost unattenuated in the pure silver specimens which have dislocation densities comparable to those in the alloys. Furthermore, the number of dislocation sites is a very small fraction of the total number of lattice positions. At a dislocation density of 10^8 per cm^2 the ratio of total lattice sites to dislocation centers is about 10^7. Thus, at 890°C, the binding energy for a probe at a dislocation would have to be over 1 eV in order that an important fraction of the probes be located there. This energy is large compared to binding energies estimated in metals at dislocations.[20] A third reason for discounting the possibility of segregation of probe ions is that such segregation should be much more extensive for the solute ions, which are present in the alloys in much larger concentrations than the probe ions and which in many cases do not fit into the silver lattice so well as In does. For example, if 50% of the In^{111} is located on dislocations, the rest of the dislocation sites in an Sb-Ag alloy should be occupied by Sb. The close proximity of the segregated Sb to the segregated In^{111} will give complete attenuation for the In^{111} nuclei involved. The rest of the In^{111} nuclei will behave in the normal way. Experimentally this effect should appear in the curve of $\hat{G}_2$ versus concentration for Sb-Ag as a displacement of the whole curve downward so that it would not extrapolate back to $\hat{G}_2=1$ at zero concentration. No such displacement appears in the curve for Sb-Ag nor in the curves for the other alloys studied. Another possibility is that a solute might segregate along dislocation lines although the probes do not. These segregated ions thus would have a distribution different from the random one assumed in interpreting the experiments. However, only a small fraction of the solute could segregate in this way because there are, relatively speaking, very few dislocation sites in the crystal. Arguments involving grain boundary segregation can be made which are very similar to the ones given here for dislocations.

In spite of the arguments there were four alloy samples which gave "hard core" attenuation for reasons that are not completely clear. Two of the samples were $\frac{1}{2}$% Au in Ag, one was $\frac{1}{2}$% Cu in Ag, and the last $\frac{1}{2}$% As in Ag. It is believed that the As and Cu results were caused by inhomogeneities in the cast billets. The two Au samples showed unusually high oxygen content and the problem with them may have been probe-oxygen association. The results quoted in this paper do not include data obtained using samples from any of these four billets.

A final experimental problem to be considered is the possibility that the bombardment of the silver alloys by 40-MeV α particles will produce activities other than In^{111} that will distort the angular correlation. A careful survey of radio isotopes produced indicates that no significant contaminant is ever present. Almost all possible candidates are eliminated by the delayed coincidence arrangement used. For example, there is no other species produced by alpha-particle bombardment of silver that involves an isomeric state with a lifetime in the range of 100 nsec. Other factors which reduce the number of contributors are the fairly long half-life necessary, the energy selection of the counters, and the small concentration of target atoms other than silver. The only prospect that has an appropriate isomeric state is Bi^{206} produced by $Ti^{203}(\alpha,n)Bi^{206}$, $Tl^{205}(\alpha,3n)Bi^{206}$, and $Pb^{204}(\alpha,pn)Bi^{206}$. It has an isomeric state of lifetime 130 nsec and a six-day half-life, but it cannot be produced in sufficient concentration to appreciably distort the correlation.

APPENDIX II: DETERMINATION OF PHASE SHIFTS

The phase shifts η_0 and η_1 listed in Table II are not the only ones that satisfy the Friedel sum rule and the resistivity relation. Other solutions will give different values of A and φ and hence different values for $\hat{G}_2$. This appendix discusses the different sets of phase shifts determined for the solutes by the Friedel sum rule and the resistivity and then describes the particular choices made in Table II.

Using the variables $y_1=\eta_0-\eta_1$ and $y_2=\eta_1$, the sum rule and resistivity expressions become

$$c_1=y_1+4y_2,$$
$$c_2=\sin^2 y_1+2\sin^2 y_2,$$

where $c_1=(\pi/2)Z'$ and $c_2=(e^2k_0/2h)(\Delta\rho/c)$. It is clear that if there is one set of solutions to this pair of equations, there will be an infinite number. For example, if $y_1=a$, $y_2=b$ is a satisfactory pair of values, so is $y_1=a+4\pi m$, $y_2=b-\pi m$ for all integral m. However, the solutions with $m\neq 0$ give the same values of A and φ as $y_1=a$, $y_2=b$. Therefore, it is necessary to look for solutions only in an interval of y_2 of length π. Usually there are two solutions in this interval.

In order to pick out the set of phase shifts which actually describes the electron scattering from a solute atom, a comparison is made with the phase shifts evaluated analytically for a particular perturbing potential. The potential is chosen to approximate the one which an electron would experience in the vicinity of a solute atom. The form chosen by us is $V(r)=(Z'e^2/r)e^{-\mu r}$. This may seem to be a strange choice considering the fact that the present paper stresses the difference between the actual potential and this form. However, the angular correlation experiments measure the potential distribution relatively far from the solute whereas the

TABLE IV. Phase shifts for potential $V(r)=(Z'_0e^2/r)e^{-1.80\ k_0r}$.

Z'_0	η_0	η_1	η_2	Friedel sum
1	1.159	0.098	0.014	0.981
2	2.407	0.240	0.029	2.107
3	3.176	0.489	0.045	3.137
4	4.042	1.107	0.063	4.937

TABLE V. Phase shifts η_0 and η_1 from Friedel sum rule and resistivity values.

Impurity	Z'	η_0	η_1	A	ϕ
Au	0.018	−0.198	0.0755	0.021	−0.052
		0.218	−0.063	0.020	+3.228
Cu	0.194	0.031	0.865	0.011	+0.094
		0.165	0.047	0.0095	+3.712
Cd	0.889	2.570	−0.392	0.031	−0.235
		0.460	0.312	0.025	+0.177
Zn	1.093	2.672	−0.319	0.025	−0.181
		0.563	0.385	0.031	+0.228
Al	1.931	3.615	−0.194	0.050	+0.099
		2.591	0.148	0.046	−0.233
In	1.826	3.525	−0.219	0.050	−0.001
		2.563	0.102	0.041	−0.338
Tl	1.713	3.528	−0.279	0.058	−0.075
		2.427	0.088	0.044	−0.492
Ge	2.978	6.551	−0.625	0.098	−0.518
		2.840	0.613	0.097	+0.490
Pb	2.584	6.140	−0.694	0.091	−0.735
		2.645	0.472	0.085	0.236
Sn	2.760	6.244	−0.637	0.089	−0.649
		2.814	0.507	0.086	0.365
As	3.918	9.263	−1.008	0.123	−1.058
		3.218	0.979	0.124	1.003
Sb	3.666	8.871	−1.038	0.108	−1.152
		3.173	0.862	0.114	0.872

phase shifts depend on the potential in the region nearer the origin. The form above has a shape near the origin somewhat similar to the one calculated by Langer and Vosko. The value of μ was chosen so that the Friedel sum rule would be satisfied approximately. It differs somewhat from the Mott value. In Table IV are the results of phase-shift calculations for $\mu=1.80\,k_0$. The Friedel sum is $(2/\pi)\Sigma_0{}^4\,(2l+1)\eta_l$, i.e., phase shifts up to η_4 are included. The values of η_2 are included in the table in order to give an idea of their expected sizes.

The independent solutions permitted by the sum rule and the resistivity values are listed in Table V. It should be noted that for Zn and Cd there are no η_0 and η_1 values that give resistivities as small as the actual ones. The tabulated values give local resistivity minima.

To make a comparison of the values in Table V with those in Table IV a plot has been constructed showing a curve of y_1 versus y_2 for the solutions in Table IV. On the same curve are the points in Table V. The solutions chosen for Table II are plotted as solid points and the others as open circles.

TABLE VI. $\hat{G}_2$ for Au and Cu using alternate phases.

Solute	Concentration	$\hat{G}_2$	η_0	η_1
Au	0.25%	0.948	−0.198	0.0755
	0.50%	0.903		
	1.00%	0.824		
Cu	0.25%	0.878	0.031	0.086
	0.50%	0.778		
	1.00%	0.625		

The choice is clear for many of the solutes. However, for Au and Cu either set of phases is equally satisfactory. Furthermore, neither Zn nor Cd fits well for either solution. The $\hat{G}_2$ for Au and for Cu have been calculated, using $\alpha=40$ and $\lambda=-70$, for the alternate phase shifts. The results are given in Table VI.

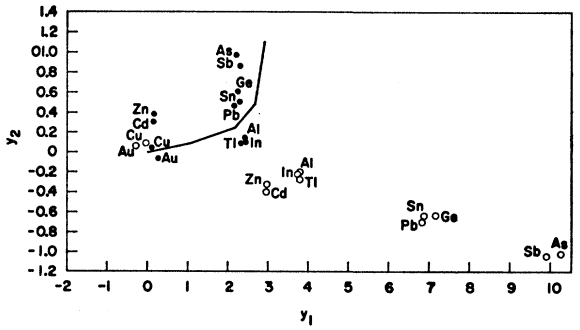

FIG. 15. The quantities $y_1=\eta_0-\eta_1$ and $y_2=\eta_1$ are plotted for each solute. The solid points are found with the phase shifts used in calculating the attenuation of the angular correlation. The open circles are alternate sets which satisfy the Friedel sum rule and the resistivity restriction. The curve connects points found by calculation using a potential of the form $(Z'_0e^2/r)e^{-1.80k_0r}$.

Notice that for both Cu and Au it makes very little difference which solution is used. The original choice for Au was made on the basis that it gives a positive η_0. This is expected for an attractive potential (positive Z') such as the one for Au. The original choice for Cu was arbitrary although it is a little closer to the curve in Fig. 15.